Confinement Improvement in High-Ion Temperature Plasmas Heated with High-Energy Negative-NBI in LHD

Y. Takeiri, S. Morita, K. Ikeda, K. Ida, S. Kubo, M. Yokoyama, K. Tsumori, Y. Oka, M. Osakabe, K. Nagaoka, T. Shimozuma, M. Yoshinuma, K. Narihara, H. Funaba, M. Goto, S. Inagaki, K. Tanaka, O. Kaneko, A. Komori, O. Motojima, and LHD Experimental Group

National Institute for Fusion Science, Toki 509-5292, Japan

e-mail contact of main author: takeiri@nifs.ac.jp

Abstract. The increase in the ion temperature due to transport improvement has been observed in plasmas heated with high-energy negative-NBI, in which electrons are dominantly heated, in Large Helical Device (LHD). When the centrally focused ECRH is superposed on the NBI plasma, the ion temperature is observed to rise, accompanied by formation of the electron-ITB. This is ascribed to the ion transport improvement with the transition to the neoclassical electron root with a positive radial electric field. In high-Z plasmas, the ion temperature is increased with an increase in the ion heating power, and reaches 13.5keV. The central ion temperature increases with an increase in a gradient of the electron temperature in an outer plasma region of ρ=0.8, suggesting the ion transport improvement in the outer plasma region induced by the neoclassical electron root. These results indicate the effectiveness of the electron-root scenario for obtaining high-ion temperature plasmas in helical systems.

1. Introduction

The Large Helical Device (LHD) is the world's largest superconducting helical device [1], and equipped with negative-ion-based neutral beam injectors (NBI) [2] and electron-cyclotron-resonance heating (ECRH) systems [3]. Using the centrally focused ECRH, high-electron temperature plasmas above 10keV have been obtained [4]. By adding the ECRH to NBI-heated plasmas, the electron internal transport barrier (electron-ITB) is formed in a core region with a steep gradient on the electron temperature profile, and improvement of the electron confinement has been observed [5,6]. This improved confinement is thought to be ascribed to suppression of the anomalous transport in the neoclassical electron root [7].

As for the ion confinement, in the tangential negative-NB injectors, the injection energy of hydrogen beam is as high as 180keV, and, thus, the plasma electrons are dominantly heated. To increase effectively the ion heating power with the high-energy NB heating, high-Z discharges with argon or neon gas-puffing are utilized, and high-ion temperature plasmas of 10keV were obtained [8]. In the high-Z plasmas, the direct ion heating power is much increased by a factor of around 5, and the ion temperature is increased linearly with an increase in the density-normalized ion heating power. That suggests the improvement of the ion transport in a sense that the power degradation of the ion temperature due to the anomalous transport is not observed.

To increase the ion temperature, the ion transport has to be improved. The present accessible approach is the improvement of the ion transport in the neoclassical electron root, in which the enhanced transport in the collisionless regime is suppressed theoretically and the anomalous transport is expected to be reduced with a positive radial electric field and its shear [9]. We have observed an ion temperature rise in the NBI plasmas superposed with the centrally focused ECRH. Then, the electron temperature profile shows the formation of the

electron-ITB, which has a centrally peaked temperature profile with a steep gradient in the core region. That suggests that the ion temperature is increased by the transition to the neoclassical electron root.

In the high-Z plasmas, on the other hand, we have increased the density-normalized ion heating power further by suppressing dilution of the high-Z plasmas with hydrogen, which has been achieved with intensive Ar and/or Ne glow discharge cleaning [10]. By enhancement of the ion heating power, the ion temperature is increased without saturation, and has reached 13.5keV. There should be the ion confinement improvement in the high-Z plasmas with high-ion temperatures.

In the followings, we present the ion confinement improvement in the electron-ITB plasmas, which are generated with the superposition of the centrally focused ECRH on the high-energy NBI plasmas. High-ion temperature experiments with the high-Z plasmas are also presented with a view of the confinement improvement. The ion transport improvement in the neoclassical electron root is discussed for the high-ion temperature plasmas.

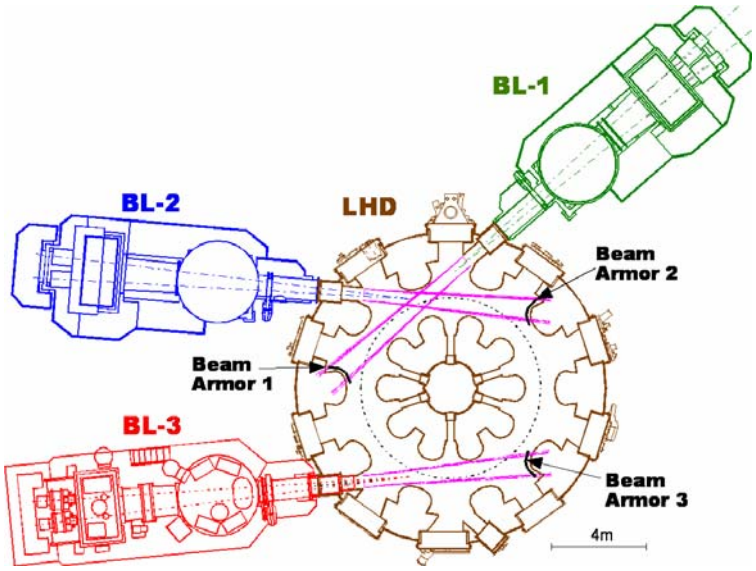

FIG. 1. Arrangement of three negative-ion-based neutral beam injectors in LHD. The injection direction of neutral beams is tangential.

2. Negative-Ion-Based NBI system and ECRH system

The neutral beam injection (NBI) system is a main heating system in the LHD, and is characterized by high-energy NB injection [2,11]. Hydrogen neutral beams with the specified injection energy of 180keV are produced through negative ions. As shown in Fig. 1, the NBI system consists of three tangential injectors, each of which has two large negative-ion sources. One injector has the opposite injection direction to the other two injectors. The injection power has gradually increased year by year since the NBI system was operational in 1998, and exceeded 13MW. The injection energy and power achieved with one injector are 186keV and 5.7MW, respectively [2,12]. High-power neutral beams are injected usually for 2-3sec with high reliability and reproducibility, and the injection duration can be extended over 100sec with a reduced power [2]. The shine-through beam, passing through the plasma

without ionisation, is incident on the beam-facing armour tiles installed inside the LHD vacuum vessel. The shine-through power is estimated with a calorimeter array on the armour tiles, and the port-through injection power is determined with the shine-through power measurement [13]. The power deposition profile of the injected neutral beams is estimated with a combination of an orbit-following Monte-Carlo calculation and analytical formulae.

The electron cyclotron resonance heating (ECRH) system employs 168GHz, 84GHz, and 82.7GHz gyrotrons, and each microwave is injected on the equatorial plane as a strongly focused Gaussian beam using vertical and horizontal antenna systems with quasi-optical mirrors [3,4]. The total injection power achieved was 2.1MW. While the injected microwaves can be concentrated within an averaged minor radius of ρ=0.2 in the inward-shifted configurations of $R_{ax} < 3.55$m, the 82.7GHz microwave is not focused on a central region of $\rho < 0.2$ in the outer-shifted configurations due to the mechanical restriction of the antenna systems. In the experiments, the second-harmonic heating with 84GHz and 82.7GHz gyrotrons is utilized. The power deposition profile is estimated with ray tracing including a weakly relativistic effect.

3. Ion Temperature Rise with Superposition of ECRH

Figure 2(a) shows the time evolution of the electron density measured with FIR and the ion temperature measured with the Doppler broadening of an X-ray line of ArXVII for an NBI plasma with a superposition of the ECRH for t=1.2-1.5s. The electron temperature profiles of the NBI+ECRH plasma (t=1.4s) and the NBI-only plasma (t=1.7s) are shown in Fig. 2(b). The magnetic axis position is 3.7m and the magnetic field strength at the center is 1.51T. As shown in Fig. 2(b), with the superposition of the centrally focused second-harmonic ECRH on a plasma heated with high-energy negative-NBI (>150keV, H), the central T_e is increased and the T_e profile has a steep gradient in a core region of around ρ=0.4, which is called an electron ITB formation in LHD [5]. Simultaneously, the central T_i is also raised with the superposition of the ECRH, as shown in Fig. 2(a). Note that an integration time for the T_i

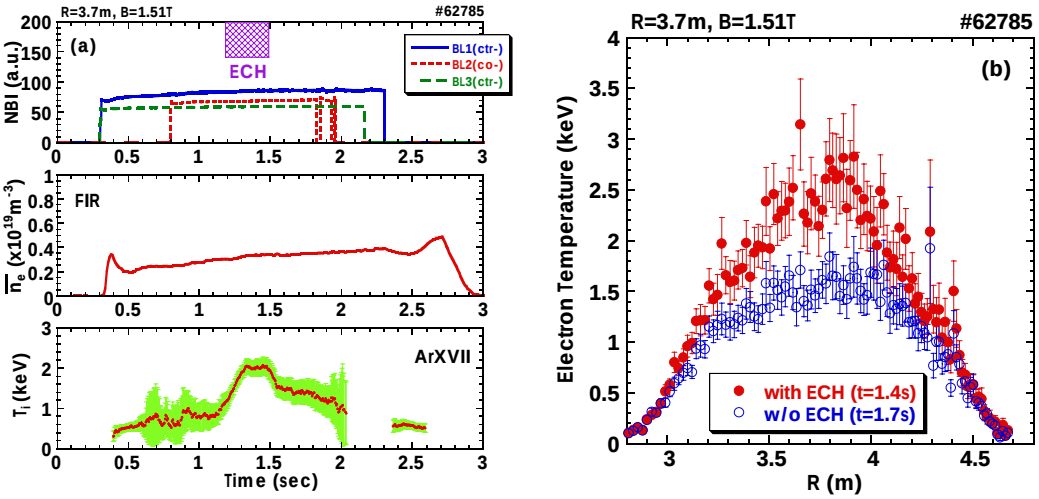

FIG. 2. (a) Time evolution of the NBI and ECRH injection timings, the n_e, and the T_i in an NBI plasma with a superposition of ECRH for t=1.2-1.5s. (b) T_e profiles of the NBI+ECRH plasma (t=1.4s) and the NBI-only plasma (t=1.7s).

measurement of 100ms should have an influence on the measured T_i-rise time. The electron ITBs in helical systems are characterized by improvement of the core electron transport due to the neoclassical electron root [7], which is in contrast with the tokamak's ITBs. The neoclassical calculation shows the formation of positive radial electric field (E_r) in the core region in the electron ITB plasma, in which the transport improvement of both ions and electrons is theoretically predicted.

The CXRS measurement was carried out for higher-density plasmas to measure the radial electric field in NBI plasmas with and without the superposition of the ECRH. Figure 3(a) shows the electron temperature profiles of the NBI+ECRH plasma and the NBI-only plasma. It is found that the electron-ITB is formed with the superposition of the ECRH. The profiles of the ion temperature and the radial electric field measured with the CXRS are shown in Figs. 3(b) and (c), respectively. A positive increase in the radial electric field is observed in a core region of ρ=0.4-0.8 with the superposition of the ECRH, and, correspondingly, an increase in the ion temperature is also observed. Since the electron density profile is not changed with the superposition of the ECRH, the NBI absorption power and profile are not so changed. Considering that the increase in the ion heating power ratio is as small as around 10% due to an increase in the T_e and that the heat exchange between the electrons and the ions is negligible, the ion temperature rise should be ascribed to the improvement of the ion transport.

The ion thermal diffusivity, χ_i, was roughly estimated for the plasmas shown in Fig. 3, with the ion temperature profile fitted parabolically toward the centre. Figure 4 shows the results of the transport analyses. Here, the thermal diffusivities for the electrons and ions are normalized by the 3/2 power of the electron and ion temperatures,

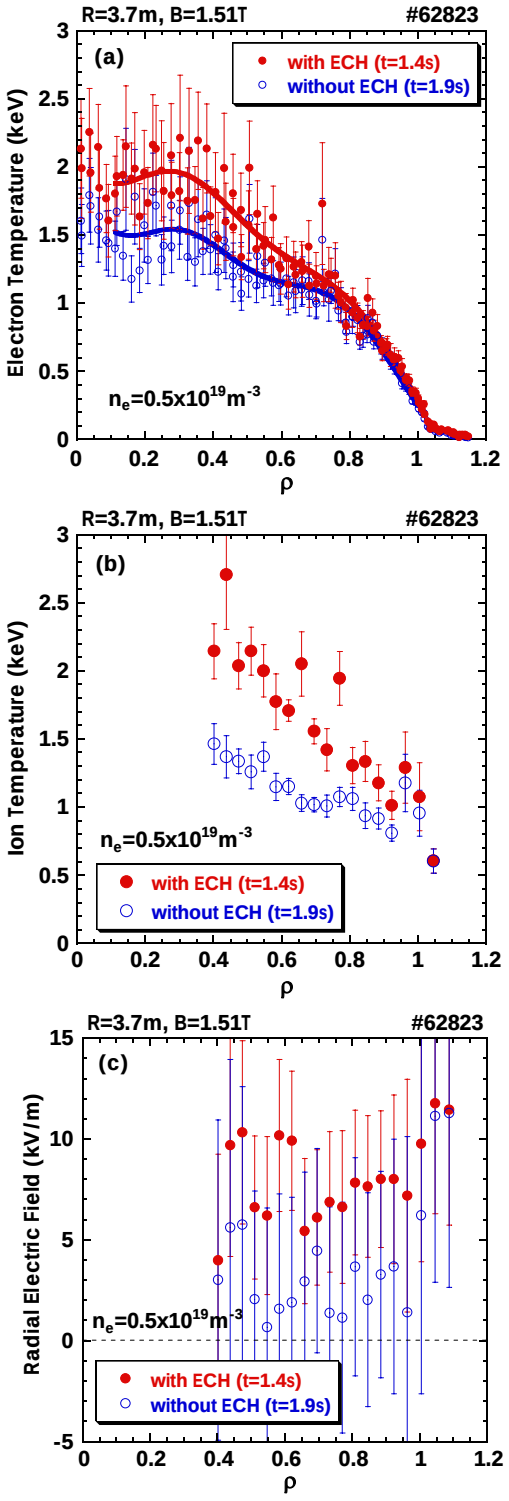

FIG. 3. (a) T_e profiles of an NBI+ECRH plasma (t=1.4s) and an NBI-only plasma (t=1.9s), and the profiles of (b) the T_i and (c) the E_r measured with the CXRS for the corresponding plasmas shown in (a).

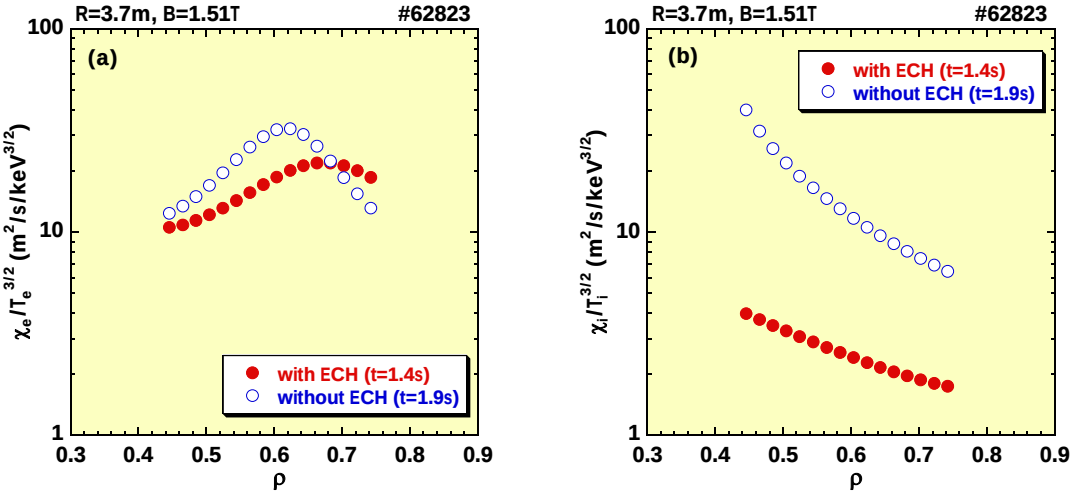

FIG. 4. Profiles of (a) the electron and (b) the ion thermal diffusivities normalized by the $T_e^{3/2}$ and the $T_i^{3/2}$, $\chi_e/T_e^{3/2}$ and $\chi_i/T_i^{3/2}$, respectively, for the NBI+ECRH plasma (t=1.4s) and the NBI-only plasma (t=1.9s) shown in Fig. 3.

respectively. The gyro-Bohm factor of $T_e^{3/2}$ is applied to the ions as $T_i^{3/2}$, and $\chi_e/T_e^{3/2}$ and $\chi_i/T_i^{3/2}$ can be used for a measure of the degree of the anomalous transport. It is found that the ion thermal diffusivity is reduced in a core region of ρ=0.4-0.7 with the superposition of the ECRH, as well as the electron thermal diffusivity. By the formation of the electron-ITB, the ion transport as well as the electron transport is improved with reduction of the anomalous transport in the neoclassical electron root.

4. High-Ion Temperature in High-Z Discharges

Although the electron heating is dominant in the high-energy hydrogen NB heating, the ion

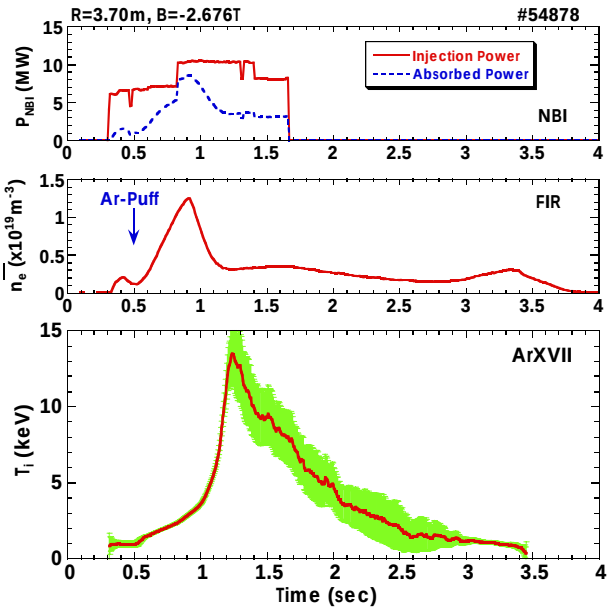

FIG. 5. Time evolutions of the NB injection and absorption powers, the n_e, and the T_i in a high-Z plasma with Ar-gas seeding.

heating is effectively enhanced in high-Z discharges with Ar or Ne seeding [8]. The ionisation (absorption) of the injected neutral beam is increased in the high-Z plasmas by a factor of around 1.5 at low-electron density plasmas below $0.5\text{x}10^{19}\text{m}^{-3}$. The ion density is reduced compared with the electron density in the high-Z plasmas. Thus, the ion heating power normalized by the ion density is much enhanced by a factor of around 5 at maximum, compared with the hydrogen-discharge plasmas. To realize these high-Z plasmas at low density, the wall conditioning by intensive glow discharge cleaning with Ar gas is effective because the high-Z plasmas are diluted with the residual hydrogen from the wall during the discharge [10]. Intensive Ar-glow discharge cleaning prior to and during a series of the high-Z experiments has been applied to reduce the residual hydrogen absorbed in the wall.

Figure 5 shows the time evolutions of the electron density and the ion temperature in an Ar-puffed plasma. The electron density is increased with the Ar gas-puffing at t=0.5s, and then decreased. The ion temperature is rapidly increased during the decrease in the electron density, and reaches 13.5 keV. In the high-Z discharges the central ion temperature is increased with an increase in the density-normalized ion heating power, and the increase in the central ion temperature is not saturated with the ion heating power. This implies that the anomalous transport causing the power degradation of the ion temperature would be suppressed in the high-T_i plasmas obtained in the high-Z discharges.

In the high-T_i plasmas, a steep electron temperature gradient is observed in an outer plasma region. Figures 6(a) and (b) show the central T_i and T_e as a function of the T_e-gradient, $dT_e/d\rho$, in an outer plasma region of ρ=0.8 and in a core plasma region of ρ=0.6, respectively. It is found that the central T_i is increased with an increase in the $dT_e/d\rho$ at ρ=0.8. The central T_e is also increased although the dependency is weaker. On the other hand, no definite correlation is observed between the central T_i and the $dT_e/d\rho$ at ρ=0.6, as shown in Fig. 6(b).

The NBI heating profile is rather broad compared with the ECH heating profile although the electron heating power is enhanced in the high-Z NBI-only plasmas. Since the helical ripple is increased toward the outer region, the transition condition to the neoclassical electron root would be mitigated in the outer region. In the neoclassical ambipolar calculation considering

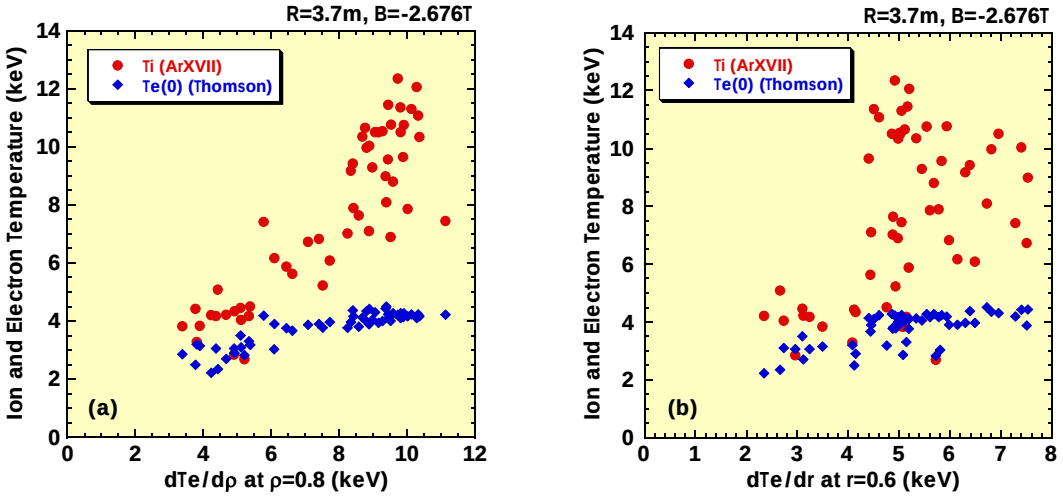

FIG. 6. Central T_i and T_e as a function of the T_e-gradient (a) in an outer region of ρ=0.8 and (b) in a core region of ρ=0.6.

multi-ion species, generation of strong positive E_r is indicated in the outer region of the high-T_i plasma, and the E_r tends to be stronger at a lower collisionality. Figure 7(a) shows the time evolutions of the electron densities and the central ion temperatures for high-Z NBI-only plasmas. The electron density at around t=1.5s is changed with variation of the Ne gas-puffing. The profiles of the radial electric field and the ion temperature, measured with the CXRS, are shown in Figs. 7(b) and (c), respectively, for the plasmas with different electron densities shown in Fig. 7(a). It is found that the positive E_r is observed in a region of ρ=0.5-0.8 and is increased as the electron density is decreased. Correspondingly, a little rise of the local T_i is also observed in the region although the central T_i is not so changed. These results of Figs. 6 and 7 suggest that the ion transport in the outer plasma region is improved due to the neoclassical electron root, and that this transport improvement should lead to the central T_i rise.

5. Concluding Remarks

An increase in the ion temperature has been observed in the high-energy NBI-heated plasmas with superposition of the centrally focused ECRH. The electron-ITB, in which the electron temperature has a centrally peaked profile with a steep gradient, is formed in a core plasma region by adding the ECRH to the NBI plasmas, and the core electron transport is improved with the transition to the neoclassical electron root. The CXRS measurement shows that increases in both the positive radial electric field and the ion temperature are observed in a core region of around ρ=0.5. The transport analysis shows that the ion transport in the core region is improved with a reduction of the anomalous transport by adding the ECRH to the NBI plasma. These results indicate that the ion temperature rise should be ascribed to the ion transport improvement in the neoclassical electron root.

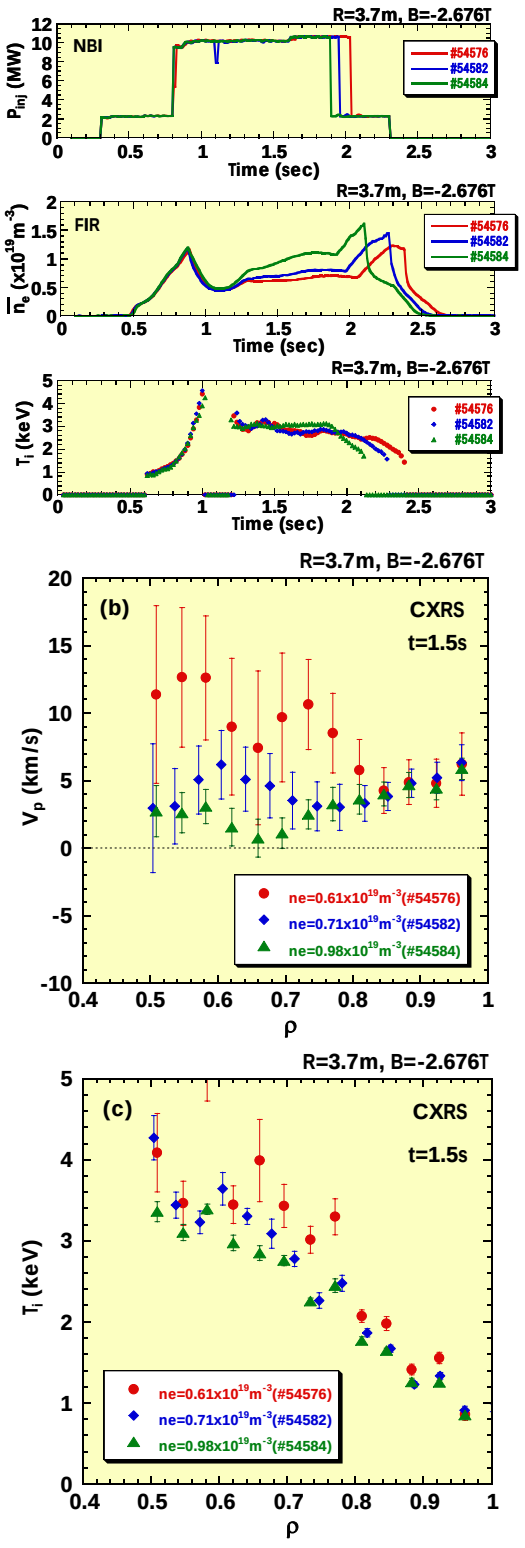

FIG. 7. (a) Time evolutions of the NB injection power, the n_e, and the T_i for high-Z plasmas with three different electron densities. (b) Poloidal rotation velocity corresponding to the E_r and (c) the T_i profiles measured with the CXRS for the plasmas shown in (a).

In high-Z discharges by Ar or Ne gas-puffing, which is realized with intensive glow discharge cleaning with Ar and/or Ne gas, the central ion temperature is increased with an increase in the density-normalized ion heating power, and reaches 13.5keV. In the high-ion temperature plasmas in the high-Z discharges, the electron temperature gradient in an outer plasma region of ρ=0.8 is related to the central ion temperature rise while that in a core plasma region of ρ=0.6 is almost independent of the central ion temperature rise. An increase in the positive radial electric field in the outer plasma region is observed with a reduction of the electron density, i.e., a reduction of the collisionality. The ion transport improvement in the outer plasma region is suggested by these results, and that should be ascribed to the neoclassical electron root.

The observation of improvement of the ion transport as well as the electron transport in the neoclassical electron root should lead to a possible scenario for obtaining high-temperature plasmas in helical systems like LHD.

Acknowledgement

The authors acknowledge all the technical staff in the LHD for the excellent operation of the LHD and the NBI and ECRH systems. This work is partially supported by a Grant-in-Aid for Scientific Research of JSPS (Japan Society for the Promotion of Science). This work has been supported by NIFS under NIFS06ULBB501.

References

[1] O. Motojima, *et al.*, Phys. Plasmas **6** (1999) 1843.
[2] Y. Takeiri, *et al.*, Nucl. Fusion **46** (2006) S199.
[3] T. Shimozuma, *et al.*, Fusion Eng. Design **53** (2001) 525.
[4] S. Kubo, *et al.*, Proc. 19th IAEA Fusion Energy Conf., Lyon, 2002, EX/C4-5Rb.
[5] Y. Takeiri, *et al.*, Phys. Plasmas **10** (2003) 1788.
[6] T. Shimozuma, *et al.*, Plasma Phys. Control. Fusion **45** (2003) 1183.
[7] Y. Takeiri, *et al.*, Fusion Sci. Technol. **46** (2004) 106.
[8] Y. Takeiri *et al.*, Nucl. Fusion **45** (2005) 565.
[9] M. Yokoyama, *et al.*, Nucl. Fusion **42** (2002) 143.
[10] Y. Takeiri, *et al.*, Proc. 20th IAEA Fusion Energy Conf. 2004, Vilamoura, 2004, EX/P4-11.
[11] O. Kaneko, *et al.*, Nucl. Fusion **43** (2003) 692.
[12] K. Tsumori, *et al.*, Proc. 20th IAEA Fusion Energy Conf. 2004, Vilamoura, 2004, FT/1-2Rb.
[13] M. Osakabe, *et al.*, Rev. Sci. Instrum. **72** (2001) 586.